SPECKLE INTERFEROMETRY WITH TEMPORAL PHASE EVALUATION: INFLUENCE OF DECORRELATION, SPECKLE SIZE, AND NON-LINEARITY OF THE CAMERA

C. Joenathan*, P. Haible, B. Franze, and H. J. Tiziani
Universitaet Stuttgart, Institut fuer Technische Optik,
Pfaffenwaldring 9, 70569 Stuttgart,
Germany

Keywords: Interferometry, Speckle Phenomena, Speckle interferometry

Abstract: Recently a new method to measure object shape, deformation, and slope of deformation using temporal evolution of speckles in speckle interferometry was reported. The principle behind the method is that certain parameter sensitive to shape or deformation is changed continuously and the fluctuations in the intensity of the speckle are recorded in a large number of frames. The phase data for the whole object deformation is then retrieved by inverse Fourier-transformation of a filtered spectrum obtained by Fourier transformation of the signal. In this paper we present a detailed theory and analyze the influence of decorrelation of the speckles on the accuracy of measurement. Further the influence of speckle size on the measurement is discussed. We also show that the method cannot only be used to measure large changes in object deformation or shape but even smaller ones with higher resolution. It is shown that the accuracy of measurement is better in the present method when compared to correlation fringe method in conventional ESPI. Further the non-linearity of the camera is shown to be useful in the enhancement of the sensitivity using temporal phase evaluation.

*Permanent address: Department of Physics and Applied Optics, Rose-Hulman Institute of Technology, 5500 Wabash Avenue, Terre-Haute, IN 47803, USA.

1.0 Introduction:

Speckle methods have been used for different deformation measurements because of several advantages and especially for the simplicity of experimental arrangement [1]. Electronic processing of the speckle interferometric pattern called Electronic Speckle Pattern Interferometry (ESPI) has enhanced the possibility of real-time with quantitative analysis [2-4]. Recently we proposed an alternate method of obtaining information about the object deformation using a method called temporal phase evaluation in speckle interferometry (TSPI) using Fourier transformation methods [5]. This basic principle of the method was then extended to measure slope of the object deformation using temporal Fourier transform speckle pattern shearing interferometry (TSPSI) [6], in-plane motion using dual beam illumination [7] and shape of an object using dual beam illumination [8]. In all these methods, a point on the object is observed over time as the object is being continuously deformed or rotated or the wavelength changed continuously. The intensity modulation of the speckles thus obtained provides the temporal evolution related to the movement or its shape. By analyzing the time dependent signal, object deformation ranging from few microns to few hundreds of microns or it shape from few hundred micrometers to few centimeters can be measured. The object deformation or slope or its shape is extracted using Fourier transformation method. The signal is first transformed, and one side of the spectrum is filtered using a band pass filter. The filtered spectrum is then inverse transformed to obtain the raw phase that is then unwrapped to get the total phase at a given point. Therefore, in principle exact linear deformation or rotation or wavelength change of the object is not necessary with this method.

In the earlier paper the basic principle of TSPI was described along with results for large object deformation measurement in the range of 100 μm [5]. Further, this idea of sequentially recording series of pattern has also been performed for shape measurement using wavelength shift [9]. In the present paper, we discuss the effect of decorrelation and speckle size on the quantitative evaluation of object deformation or its shape or slope of deformation. The inherent non-linear property of the CCD

camera is shown to be useful in the enhancement of the sensitivity of the measurement. It is also shown that the method can be extended to measure small deformations with higher accuracy when compared to the conventional ESPI method.

2.0 Principle of temporal phase evaluation:

The schematic diagram of one of the speckle interferometric arrangement is shown in Fig. 1. This arrangement (TSPI) is used for the measurement of out-of-plane deformation of the object. A He-Ne laser beam with a power of 30 mW was expanded with a spatial filtering set up and then collimated to obtain a beam of 30mm diameter. In order to test the principle of the method as well to make the discussion in this paper easy we use rotation of an object. A metal plate was mounted on a computer controlled rotational stage and tilted by a small angle about the x-axis producing z-axis displacement linearly varying along the y-axis.

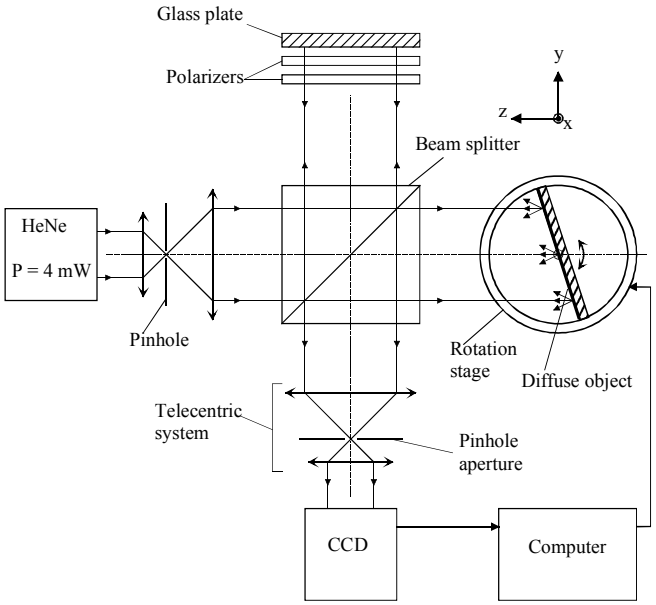

Fig. 1: Schematic of the experimental arrangement of the temporal Fourier-transform speckle interferometric method.

The intensity of the reference beam was adjusted with the help of two polarizers to either match or exceed the intensity of the object beam. The collimated laser light is split into two beams using a beam splitter. One beam illuminates a diffuse object and the other is reflected from a mirror forming the reference beam. This configuration is similar to that of the Michelson interferometer. The reference arm and the object arm are set to have arbitrary path length from the beam splitter. A telecentric system is used to focus the object onto the sensor of a high speed Charge Coupled Device (CCD) camera. In addition, the telecentric system insures the propagation axis of the beam from the mirror and the object to be collinear. The intensity of the interference signal observed at the sensor plane can be expressed as

$$I(x,y,t) = I_o(x,y)\left\{1 + m\cos\left[\Phi_0(x,y) + \Phi(x,y,t)\right]\right\} \quad (1)$$

Where $I_o(x, y)$ is the bias intensity in the complex interference pattern formed between the object and reference beam, m is the modulation of interference pattern, $\Phi_0(x, y)$ is the random phase of a speckle, and $\Phi(x, y,t)$ is the position and time dependent phase introduced due to out-of-plane or in-plane or the slope of the object deformation or the shape of the object. The relationship for $\Phi(x,y,t)$ depending on the setup used is

$$\Phi(x, y, t) = \frac{4\pi h(x, y)\,\Delta\lambda(t)}{\lambda^2}\,[\text{shape}] \quad 2(a)$$

$$\Phi(x, y, t) = \frac{2\pi W(x, y, t)\,(1+\cos\theta)}{\lambda}\,[\text{out - of - plane}] \quad (2b)$$

$$\Phi(x, y, t) = \frac{4\pi [U(x, y, t), V(x, y, t)]\sin\theta}{\lambda}[\text{in - plane}] \quad (2c)$$

$$\Phi(x, y, t) = \frac{4\pi(\partial W(x, y, t)/\partial x)\Delta x}{\lambda}[\text{slope}] \quad (2d)$$

$$\Phi(x, y, t) = \frac{4\pi [h(x, y)]\sin\theta\Delta\theta(t)}{\lambda}[\text{shape}] \quad (2e)$$

The first equation 2(a) represents the method used for measuring shape using wavelength shift [9], equation 2(b) is used in out-of-plane sensitive conventional speckle interferometry where the angle of object illumination is θ, equation 2 (c) corresponds to the measurement of in-plane displacement in a dual beam illumination optical configuration, U, V, and W

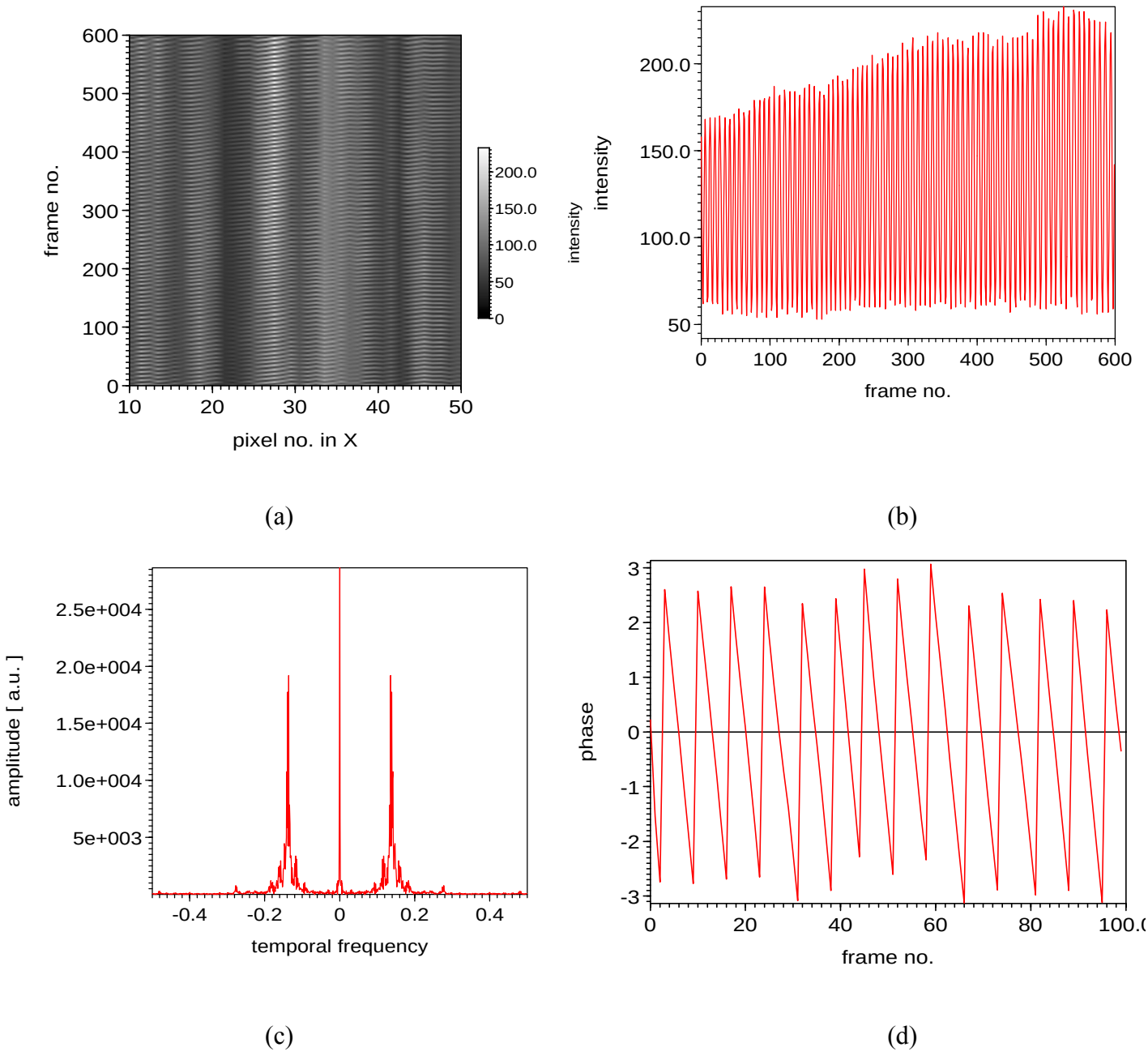

Fig. 2: Experimental results for an object tilted continuously. (a) A slice of one horizontal line of pixel from each frame stacked together. Only 600 of the 1024 frames are shown to clearly depict the speckle modulation and the correlation. (b) The intensity variation of one speckle as a function of time. (c) The Fourier-transformation of the temporal signal shown in (b). (d) The inverse Fourier transform of the filtered spectrum. The phase varies between $-\pi$ and $+\pi$ and only 100 frames are shown for clarity.

are the displacement components along the x, y, and z directions respectively, equation 2 (d) is for shear interferometric arrangement, Δx and Δy are the amount of shear along the x and y directions respectively in the shearing interferometer, and for the TSPSI setup the angle of object beam illumination is zero, equation 2(e) is for shape measurement in a dual beam illumination setup, and $\Delta\theta$ is the angle of rotation which is time dependent. Let us consider one point on the image of the object and as the object is deformed or rotated or the wavelength changed, the intensity fluctuation is recorded as a function of time. The instantaneous temporal frequency of the signal observed at a given point of the image of the object during 't' seconds of recording is

$$f_{ins}(x, y, t) = \frac{1}{2\pi ë} \frac{\partial \Phi(x, y, t)}{\partial t} \quad (3)$$

Thus the temporal frequency of the signal observed is dependent on the object deformation or its slope or the object height. A large number of frames of the speckle pattern are recorded sequentially as the object is being deformed. For each pixel we observe the speckle intensity variation over time providing the pixel history. Figure 2 (a) shows one such figure of the speckle modulation of a horizontal line from each frame stacked over for 600 frames. The intensity oscillation observed at a given pixel is shown in Fig. 2 (b). By taking the Fourier-transform with respect to the time variable of each pixel history (Fourier Transform of equation 1 after further simplification) we obtain

$$F\{I(x, y, t)\} = \tilde{A} + \tilde{B}(f - f_{med}) + \tilde{C}(-f - f_{med}) \quad (4)$$

Where

$$\tilde{A} = F\{I_0(x, y)\},$$

$$\tilde{B}(f - f_{med}) = F\left\{\frac{I_0(x, y)}{2} m \exp[i(\Phi o(x, y) + \Phi(x, y, t))]\right\},$$

$$\tilde{C}(-f - f_{med}) = F\left\{\frac{I_0(x, y)}{2} m \exp[-i(\Phi o(x, y) + \Phi(x, y, t))]\right\},$$

F stands for Fourier transform, and f_{med} is the median frequency of the signal generated. Equation 4 shows two bands are obtained on either side of a central peak in the Fourier spectrum and is shown in Fig. 2 (c). The carrier frequency generated due to the object displacement or other changes should be large enough to separate the side bands from the central peak. Upon isolation of one of the side bands with an appropriate band pass filter, an inverse Fourier transform is applied to the filtered spectrum, thus giving rise to a complex term as

$$F^{-1}\{\tilde{B}(f - f_{med})\} = C_1 \frac{I_0(x, y)}{2} m \exp[i(\Phi o(x, y) + \Phi(x, y, t))] \quad (5)$$

Where C_1 is a constant introduced by the transformation. From the angle of the complex values of the resultant transform, the phase information is extracted. The initial phase is eliminated if the difference between the first frame and the last frame is taken. This procedure of obtaining the phase does not demand that the displacement be linear. For non-linear deformations the side bands broaden demanding that the width of the band pass filter used must be changed appropriately. The raw phase data obtained after inverse Fourier transforming the filtered spectra is exhibited in Fig. 2 (d). This phase is then unwrapped as in phase shifting interferometry giving the total phase at that point. Obtaining the phase at all the points of the object provides the 3-D map of the time dependent phase of the object deformation. From the 3-D data, the beginning and the end phase of the object deformation can be obtained. In the present method of analysis, the instantaneous angular frequency or the linear velocity generated during deformation of the object point is determined. From these extrapolations the 3-D plot of the object deformation is extracted.

If the deformation or the rotation or the wavelength shift is kept linear, then the separation of the side band from the central peak can be used to determine the number of cycles and thus the total phase in the time of acquisition of the data. It will be shown later that the non-linearity of the camera can be used in these cases to enhance the measurement resolution by looking at higher orders in the Fourier spectra.

3.0 Decorrelation:

3.1 Simulation:

In the above analysis the modulation in equation 1 is inherently assumed to be constant during the time of acquisition. However, it is well known that the longitudinal speckle size is limited and has a cigar shape. Speckle intensity as the object is deformed increases gradually starting from zero at the beginning of the structure. Finally the speckle intensity becomes

zero at the end of the structure. Figures 3 a) and 4 a) show that signal modulation in our experiments. It is interesting to note that the signal is present even after the speckle has passed through. The plots were obtained by scanning one horizontal line from each frame staked together and only a section of the 1024 frames are displayed for clarity. By scanning many of the experimental results of the TSPI data it was found in most of the cases the transition from one speckle to another was gradual as can be seen in the examples. The overall intensity variation of the cigar shaped speckle is well known in the literature and is determined from the autocorrelation of the intensity in space [10] which is $\sin(\Phi_M)/\Phi_M$ where Φ_M is the phase in the speckle which is a function of the Z-component that is along the beam propagation. This leads to correlation length which is the average grain width in the direction of observation and is $8\lambda(L/D)^2$, where D is the width of the illumination beam and L is the distance of observation from the diffuser. The interference equation with the presence of the intensity variation in the speckle therefore is

$$I(x, y, t) = a_1^2 + a_2^2 \operatorname{sinc}^2(\Phi_M) + 2a_1 a_2 \operatorname{sinc}(\Phi_M) \cos\left[\Phi_0(x, y) + \Phi(x, y, t)\right] \quad (6)$$

Where a_1 and a_2 are the amplitudes of the reference and object beam and $\operatorname{sinc}^2(\Phi_M)$ is the modulation of the intensity of the cigar shape structure of the speckle in the speckle pattern. The plots of the above equation with some arbitrary values for the phase and with the object to reference beam ratio of 1:9 are shown in Fig. 3 b). Similarly Fig. 4 b) is the simulation of the modulation for Fig. 4 a) and with an object to reference beam ratio of 1:4 matches well with the experimental results.

3.2 Error in the phase due to decorrelation:

It is also important to determine if the speckle intensity variation introduces any error in the calculation of the phase with the Fourier transform analysis. Equation 6 can be further simplified to a form as

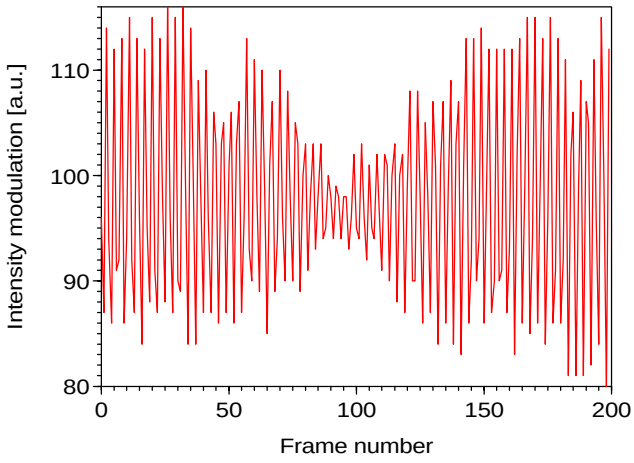

(a)

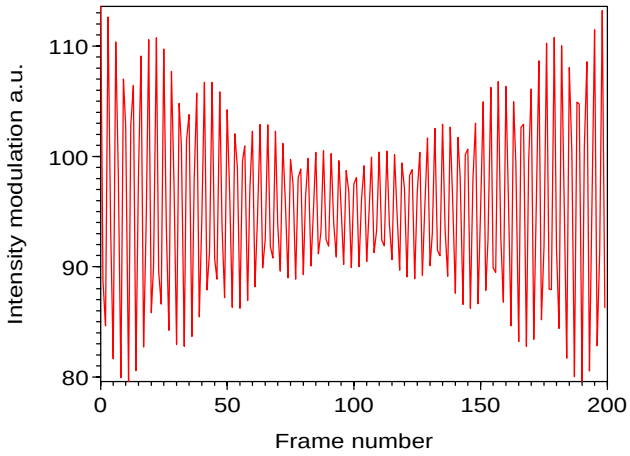

(b)

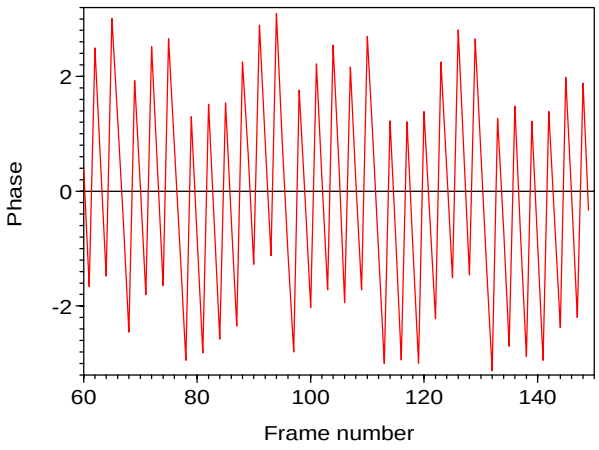

(c)

Fig: 3: The signal modulation at one pixel against frame number and only 200 of the 1024 frames is shown. a) The experimental modulation near the transition region from one speckle to another. b) Theoretical plot of the intensity variation of two-cigar shape structure for the speckles. The object to reference beam ratio was taken to be 1:9. The phase of the speckles and the intensity of the beams were so set to match the experimental results. c) The phase plot obtained with the Fourier transform method of analysis, which exhibits no odd phase jumps in the transition zone. Odd jumps do occur at some transition zone if no signal is present.

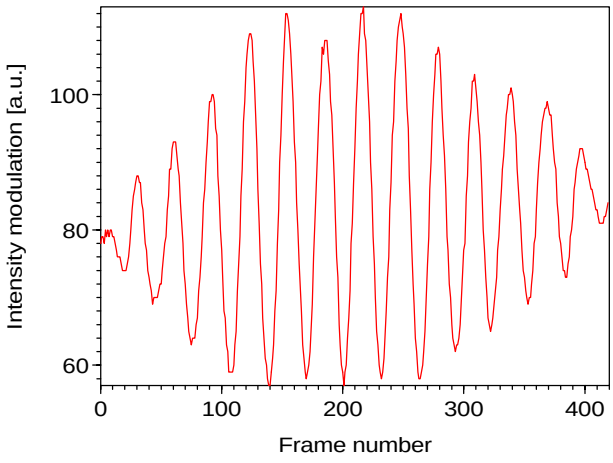

(a)

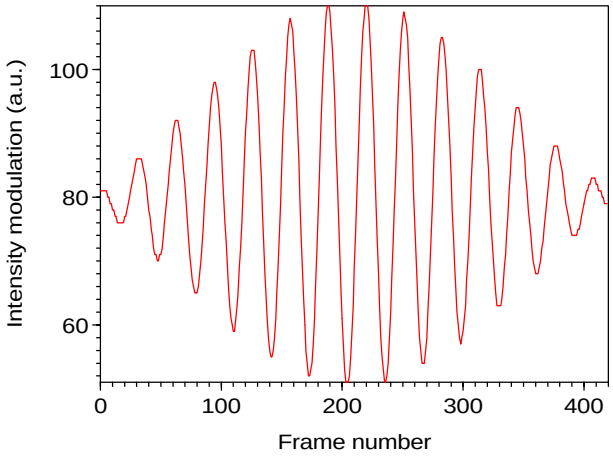

(b)

.

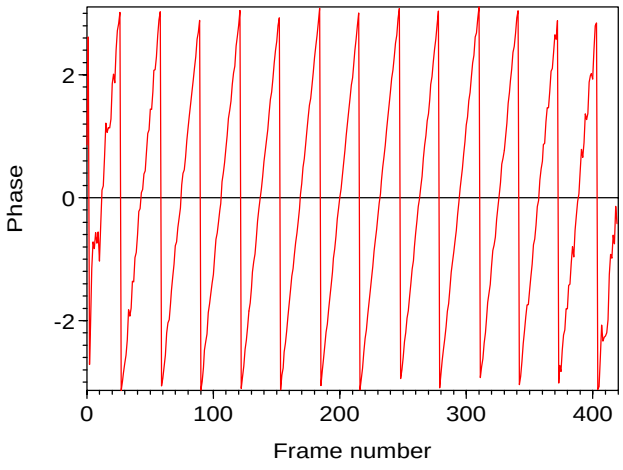

(c)

Fig. 4: The signal modulation in one speckle and 400 of the 1024 frames are shown. a) The experimental modulation taken from a data for an object deformed during the exposure. b) The theoretical plot where the object to reference beams was taken to be 1:4 respectively. c) The raw phase plot obtained with the speckle intensity modulation matches the results with no speckle modulation.

$$I(x, y, t) = a_1^2 + a_2^2 \mathrm{sinc}^2(\Phi_M) + 2a_1 a_2 \left[\frac{\sin(\alpha + \beta)\Phi}{2\alpha\alpha} + \frac{\sin(\alpha - \beta)\Phi}{2\alpha\alpha} \right] \quad (7)$$

Where $\Phi_M = \alpha\Phi$, $\Phi_o + \Phi = \beta\Phi$, α and β are proportionality constants. Applying, Fourier transformation of the signal [present in the form of eqn. (7)] the spectra obtained is found to be modified by the presence of sinc (Φ_M), in other words under ideal conditions two top hat spectra are obtained where one is displaced by f_M and the other by $-f_M$ (where f_M is the frequency created by the speckle intensity variation) from the center. However, due to frequency changes caused by nonlinear deformation of the object or wavelength shift, the side peaks are broadened. Phase changes caused by the second term in eqn. 7 is small and lies close to the central peak in the Fourier transform plane. Usually, the frequency f_M caused by the speckle intensity variation is quite small compared to the frequency of the signal and thus the side spectra contains two bands that cannot be separated. If f_M is small then the maximum lies at f_{med} (the frequency peak obtained without the presence of the speckle intensity variation) since the two side bands are displaced symmetrically by $+f_M$ and $-f_M$. If the median frequency of the signal is extracted then no error is introduced due to the speckle.

In our method of analysis, using an appropriate bandpass filter, one of the side band is filtered. It should be noted that if the second speckle following the first one does not appear then the signal modulation is zero in the transition region. This causes additional phase jumps in the transition zone to appear thus introducing error in the calculation of the total phase which is generally small compared to the total phase introduced due to object deformation. The signal in Fig. 3 a) was processed using the Fourier transform procedure described in section 2.0 to obtain the phase values and Fig. 3 c) depicts the phase values near the transition zone from one speckle to the other. There appears no odd phase jump in the region of the transition zone. However, as the phase of the speckle is random, near the transition zone from one

speckle to another there are odd phase jumps. Further, when the signal is not present in the transition zone or for signal modulation close to the quantization level of the pixel then additional error is introduced. Figure 5 (b) shows the phase plot for a pixel with odd jumps in the phase where signal modulation is absent in the transition zone from one speckle to the other [Fig 5 (a)].

Error caused by such jumps can be minimized if the phase is unwrapped and compared to the value of the phase to the adjacent pixel. Odd phase jumps can be observed to cause abnormal changes in the slope of the unwrapped phase plot and therefore can be easily spotted and reduced considerably. Another simple and straightforward method that we have successfully adopted is by using a narrow bandpass filter to extract one of the side bands. Thereby only regions close to the median frequency is filtered. This not only preserves the phase fluctuation in the region of the signal but also introduces an average signal modulation in the region of no signal and this is shown in Fig. 5 (c). One can see that the odd phase jumps encountered in Fig. 5(b) where a broad bandpass filter was used have been reduced considerably. In general it can be concluded that as long as a signal is present in the region of decorrelation, the phase information extracted is without any influence from the modulation created by the decorrelation term. A narrow bandpass filter was found to work very well when more than one longitudinal speckle length was used for measurement.

4.0 Multiple/Spurious reflections:

In addition to the longitudinal speckle size that influences the signal, multiple reflections or spurious reflections in these interferometers creates additional secondary modulations. The interference equation with spurious modulation is

$$I(x,y,t)=I_o(x,y)\{1+m_1\cos[\Phi_o(x,y)+\Phi(x,y,t)]+m_2\cos[\Phi_2(x,y)]\} \quad (8)$$

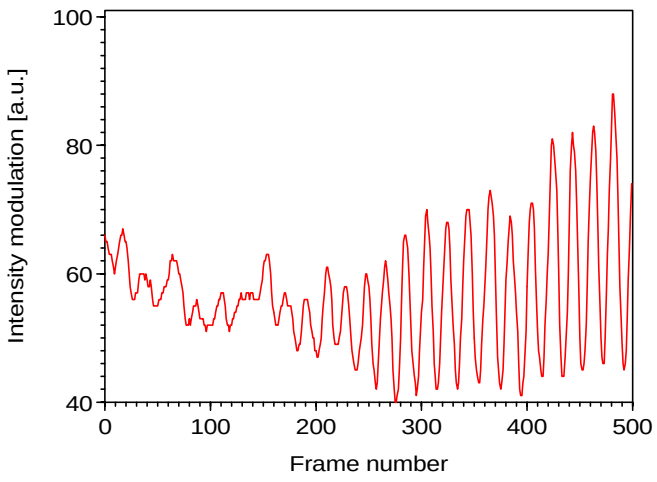

(a)

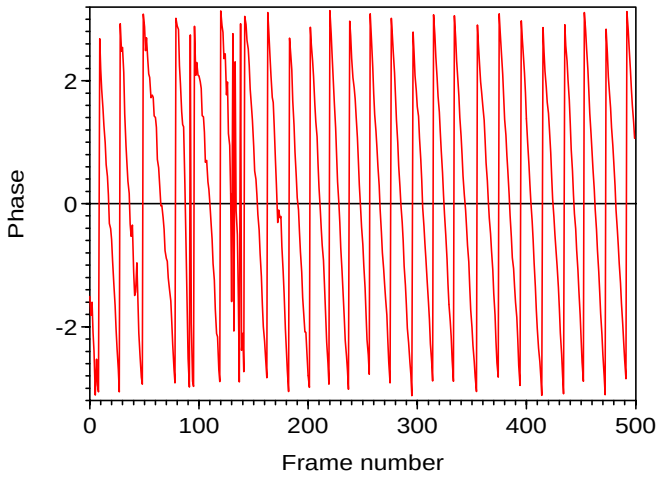

(b)

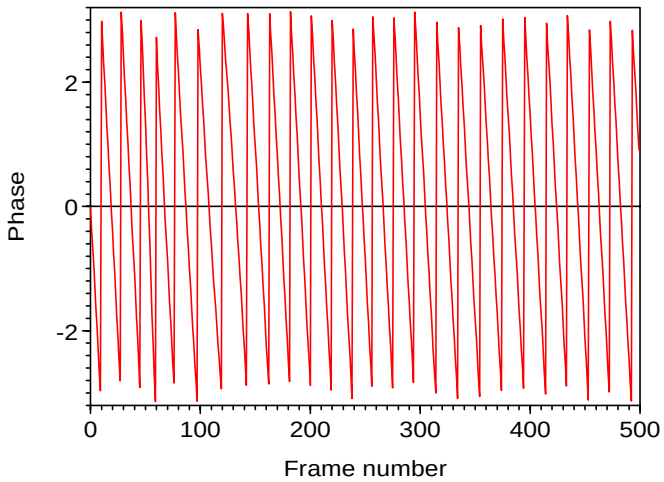

(c)

Fig. 5: The effect of the width of the bandpass filter in retrieving data in the transition zone when no signal is present. a) The signal modulation is reduced considerably at the beginning and then is good after 200 frames. b) The raw phase plot obtained with a broad bandpass filter. Odd phase jumps occur in the region of poor signal. c) The raw phase map with a narrow bandpass filter centered close of the peak in the side band.

Where m_1 and m_2 are the signal and spurious reflection interference modulation, and Φ_2 is the phase of the spurious signal. If the secondary modulation caused by spurious reflections in the interferometer is of a higher frequency than the signal bandwidth, then other peaks appear in the Fourier spectrum. Secondary modulations with frequency identical to the signal or in multiples do not cause any error but enhances signal detection. On the other hand if the secondary modulation lies in close proximity of the signal frequency then the combined spectrum is extracted for analysis thereby introducing error in the phase evaluation.

5.0 Influence of speckle size:

It is usually assumed that the speckle size σ be matched to the pixel size ρ to obtain high signal modulation. In general the speckle size is controlled by an aperture placed before or after an imaging lens and in the case of a telecentric imaging system it is placed before the second lens. If the demagnification of the imaging system is M, then information from a region of σ/M (also ρ/M) in the object is averaged over one speckle. If we assume that n number of speckles fill one pixel, the information again in a region of σ/M is averaged in the pixel. The modulation of the combined signal from n number of speckles in one pixel can be expressed as

$$I_T(x, y, t) = \sum_{i=1}^{n} \left(A_i + B_i \cos\left[\Phi_{0i}(x, y, t)\right]\right) \qquad (9)$$

Where $A_i = a_{si}^2 + a_{ri}^2$, $B_i = 2\, a_{si}\, a_{ri}$, Φ_{0i} is the random phase of the i th speckle, a_{si} is the intensity of the i th speckle and a_{ri} is the part of the reference beam that interferes with the i th speckle. The reference beam at the given pixel is $R = \Sigma\, a_{ri}$ and the total object beam due to all the speckle is $O = \Sigma\, a_{si}$. As the speckles are spatially isolated it has been assumed in the above equation that the intensity of the reference beam is divided equally between the number of speckles in a given pixel. Usually in speckle interferometry, the intensity of the reference and object beams are adjusted to be equal and most often the reference beam is slightly greater than the object beam. The modulation m_i of the i th speckle from the above equation is B_i / A_i. The modulation of the speckle caused by object displacement or movement or wavelength change is high if the portion of the reference beam equals the i th speckle intensity. However, the overall modulation at the pixel due to the combined speckle modulation is reduced and is dependent on the random phases of the individual speckles in the given pixel. As the phase of the speckles are uniformly distributed between $-\pi$ and $+\pi$, there exists certain pixel where the signal modulation will be greatly reduced due to phase mismatch between the speckles in the pixel. Moreover as the probability of two neighboring speckles to have the same intensity is quite small, the overall modulation observed at a pixel will not be zero even if the neighboring speckles are at out of phase by π degrees.

If we assume that there are two speckles at a pixel, then the signal can lie anywhere between 1 and above zero with a high probability being 0.5. Therefore, information can be extracted from almost all the pixels. Fourier transformation of the above signal results in four side bands with two bands on either side of the central peak. The two bands on one side are then centered over frequencies f_1 (due to the modulation created from one speckle) and f_2 (due to the other in the same pixel). As the speckles projected onto the object are spaced of the order of 80 μm, the frequency difference is small compared to the width of the bands and therefore cannot be separated. Therefore, the final phase value calculated after inverse Fourier transformation is the average value of the displacement or shape or slope information in the two speckles. The result is similar to the value obtained if the speckle size is matched to the pixel size.

Since the speckles do not overlap in a given pixel, the cross interference term in the above equation has been left out. If the intensity of the object is matched to the reference beam as is usually done in interferometry, then the individual modulation of the speckles is close to unity. The overall maximum modulation of the combined signal due to the initial phases of the speckle, which is random, will then be reduced. For odd number of speckles in the pixel, the probability of the signal modulation to be zero is quite small. This is due to the fact that the even if

two speckles are out of phase then the modulation from the third speckle is retained as the pixel modulation. However, it should be noted that the signal modulation should be more if not in some multiples of the quantization value used in transforming the analog signal to digital signal. Figure 2 a) shows the signal when the speckle size is matched to the pixel size. The aperture of the imaging system was increased to obtain two speckles in one pixel and Fig. 6 a) and b) show signal modulation at two adjacent pixels. The signal modulation is reduced drastically in Fig. 6 b). As the average intensity in the two pixels is the same, the cause for the reduced signal modulation in one pixel should be the phase mismatch between the two speckles in the pixel. Further, the experiment was carried out by increasing the aperture to have the possibility of three speckles in one pixel. However, the signal modulation was consistently found to be low but always higher than in the case of two speckles in one pixel. Pixels where the signal modulation is close to the quantization level of the camera used will produce no data and usually has been eliminated in our analysis by using a spike only type filter (spike filter) [5-8].

It should be noted that larger aperture would reduce the cigar shape (longitudinal) length of the speckles. But as more than one speckle is present in the pixel there exists a greater chance of another speckle appearing and therefore the overall modulation of the signal will remain relatively uniform unlike in the case of one speckle covering a pixel.

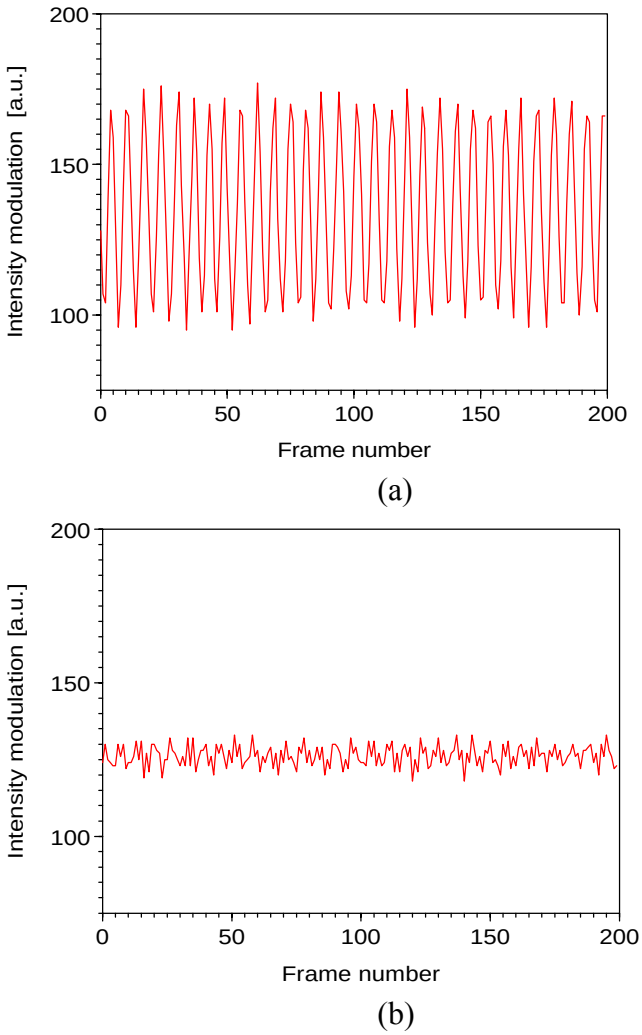

Fig. 6: The effect of the number of speckles in one pixel. Here two pixels were taken to fill one pixel. Only 200 of the 1024 frames are displayed. a) The signal modulation obtained in one pixel is good and well above the quantization level of the camera. b) However, the signal modulation in the adjacent pixel is reduced considerably in spite of the high average intensity. This reveals that the phase difference in the two speckles is π.

6.0 Non linearity of the camera

In our earlier work we have assumed that the camera response to the intensity is linear. However, the CCD camera in general has a non linear response to intensity and can be expressed as

$$V(t) = C + \alpha I(t) + \beta I^2(t) + \gamma I^3(t) + \ldots \qquad (10)$$

where C, α, β, and γ are constants. Substituting for intensity from equation 1, equation 11 reduces to a form as

$$V(x, y, t) = K_o + K_1 \cos[\Phi_o + \Phi(x, y, t)] + K_2 \cos 2[\Phi_o + \Phi(x, y, t)] + K_3 \cos 3[\Phi_o + \Phi(x, y, t)] + \ldots \qquad (11)$$

Where K_o, K_1, K_2, and K_3 are constants after simplifying equation 10. This shows that upon Fourier transformation higher order peaks are obtained that can be used to increase the resolution of the method. However, the signal to noise ratio in the higher order side bands is low. Using a band filter if a higher order band can be filtered then the resultant phase in the case for example out-of-plane sensitive interferometer is

$$\Phi(x, y) = \frac{4 N \pi \Delta Z(x, y)}{\lambda} \qquad (12)$$

Where N stands for the order number. In the shape measurement using wavelength shift, for linear shift in the wavelength the frequency of the signal can be directly related to the height of the object point. The resolution with linear displacement or linear shift in the wavelength can be increased by choosing the appropriate order. Figure 7 shows the peaks obtained in the Fourier transform plane for a signal modulation close to the saturation level of the camera. Two peaks are obtained showing that the second peak is due to the non linearity of the camera. The camera setting was not changed and set to operate in the linear region.

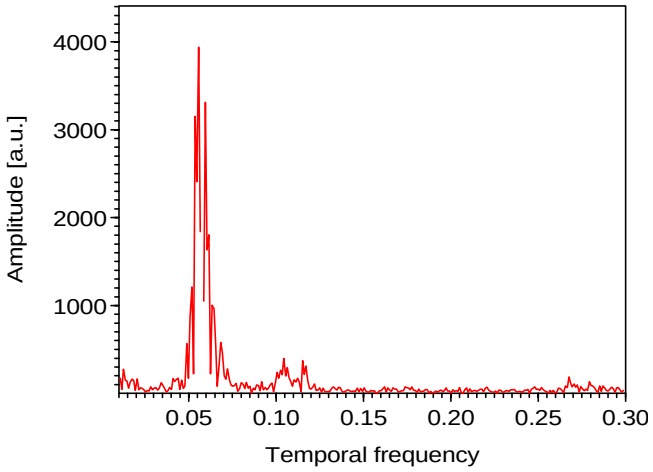

Fig. 7: The spectra obtained in the Fourier transform plane. The second peak is due to the nonlinear response of the camera and is the second order term in the nonlinearity

7.0 Range of measurement:

It is clear that points on the object with zero displacement cannot be resolved because no side band are generated. Also for points where 10 cycles (this width is set by the width of the side band) or less modulation is generated, a resolvable separation of the side band from the central peak in the spectrum is not obtained. Therefore, these points of the image do not have any data. This resolution is dependent on the band-pass filter used to separate one of the side order bands. To overcome this problem we have introduced a constant displacement or slope based on the sensitivity of the method. This modification introduces a reference temporal frequency signal (off-set), which modifies equation (1) to

$$I(x, y, t) = I_o(x, y)\left\{1 + m\cos\left[\Phi_o(x, y) + \Phi_1(t) + \Phi(x, y, t)\right]\right\} \qquad (13)$$

Where the phase factor $\Phi_1(t)$ is a constant and contains the reference frequency off set. Consequently with no object displacement there is a reference frequency. However, if the non linearity of the camera were to be used, then displacements that create less than 10 cycles can also be resolved. The accuracy of measurement for small displacements with the present method is quite high compared to the ESPI method. Assuming that 10 cycles of constant displacement and 10 cycles due to object deformation, the accuracy of displacement measurement is close to $\lambda/50$ at that point for out-of-plane displacement measurement. Such high accuracy cannot be attained with ESPI method because a low pass filter is necessary to eliminate speckle noise. In the case of the shearing the accuracy on the smallest slope that can be determined is dependent on the shear used. However, the accuracy is much better than the shearing fringes obtained by correlation. In the case of contouring using dual beam illumination, the number of cycles that can be recorded is based on the speckle size. Assuming the pixel size to be 16 μm, the number of cycles that can be recoded is 350. Therefore, for an object height of 5mm, the height resolution that can be obtained is 15 μm.

Another factor of interest is the upper limit on the displacement or slope that can be measured is set by the maximum number of cycles that can be recorded in the total number of frames. This theoretical upper limit is set by the Nyquist criterion. This limit is

$$h(x, y) = \frac{N_{nq}\,\lambda^2}{\Delta\lambda} \text{ [shape by wavelength shift]} \qquad (14a)$$

$$Z(x,y) = N_{nq}\frac{\lambda}{1+\cos\theta} \text{ [out-of-plane displacement]} \qquad (14b)$$

$$U(x, y), V(x, y) = N_{nq}\frac{\lambda}{2\sin\theta} \text{ [in-plane displacement]} \qquad (14c)$$

$$\frac{\partial Z(x, y)}{\partial x}\Delta x = N_{nq}\frac{\lambda}{2} \quad \text{[Shear interferometry]} \qquad (14d)$$

$$h(x, y) = \frac{N_{nq}\,\lambda \sin\theta \Delta\theta}{2} \quad \text{[Shape by dual beam illumination]} \qquad (14e)$$

Where N_{nq} is the Nyquist frequency and in our set up is 512 cycles. Increasing the total number of frames that is recorded can increase the upper limit. It should also be kept in mind that a reference frequency off set is sometimes necessary and this will cut down on the maximum number of cycles used for measurement.

8.0. Conclusion:

We have discussed in this paper the effect of decorrelation and multiple reflections on the measurement in temporal phase evaluation speckle interferometer (TSPI). In the method large number of frames of the object motion is recorded and then analyzed using Fourier transformation procedure. It was shown that the intensity variation in the longitudinal speckle size as well as the secondary modulations arising due to multiple and spurious reflections do introduce error in the determination of the phase. Two simple methods were proposed to reduce error in the case of measurement exceeding the longitudinal speckle size. In one method the width of the band pass filter was appropriately reduced and in the other the phase change between two pixels was compared in the wrapped phase plot. Speckle size was found not to influence the final results as long as modulation obtained was above the quantization level of the camera. The accuracy in the case of small deformations is comparable to conventional ESPI systems if not a magnitude better and the upper limit on the deformation is up to a 500 μm. The nonlinearity of the camera is shown to generate higher order peaks in the Fourier spectra and therefore can be used effectively to enhance the range of measurement.

Acknowledgments: The authors gratefully acknowledge the financial support by the 'German Research Association' DFG.

9.0 References:

1. K. Erf, Speckle Metrology, Academic Press, New York, 1978
2. R. Jones and C. Wykes, "Holographic and Speckle Interferometry," Cambridge University Press, London, 1983
3. R. S. Sirohi, "Speckle Metrology," Marcel Dekker, New York, 1993
4. C. Joenathan, "Speckle Photography, Shearography, and ESPI," in Optical Measurement Techniques and Applications, ed. P. K. Rastogi, Artech House Inc, Boston, London, 1997
5. C. Joenathan, B. Franze, P. Haible, and H. J. Tiziani, "Speckle interferometry with temporal phase evaluation for measuring large object deformation," In press, Applied Optics, 1998.
6. C. Joenathan, B. Franze, P. Haible, and H. J. Tiziani, "Large in-plane displacement measurement in dual beam speckle interferometry using temporal Fourier-transformation," In press, J. Modern Optics, 1998.
7. C. Joenathan, B. Franze, P. Haible, and H. J. Tiziani, "Novel temporal Fourier transform speckle pattern shearing interferometer," In press Optical Engineering, 1998
8. C. Joenathan, B. Franze, P. Haible, and H. J. Tiziani, "Shape measurement using temporal Fourier-transform in dual beam illumination speckle interferometry," In press, Applied Optics, 1998.
9. H. J. Tiziani, B. Franze, and P. Haible, "Wavelength-shift speckle interferometry for absolute profilometry using a mode-hop free external cavity diode laser," J. Mod. Opt, 44, 1485-1496 (1997)
10. L. Leushacke and M. Kirchner, "Three-dimensional correlation coefficient of speckle intensity for rectangular and circular apertures, J.O.S.A.A, 7, 827-832 (1992)